Cellular and Molecular Life Sciences (2022) 79:99
https://doi.org/10.1007/s00018-021-04097-x

ORIGINAL ARTICLE

PRMT7 ablation in cardiomyocytes causes cardiac hypertrophy and fibrosis through β-catenin dysregulation

Byeong-Yun Ahn[1,3] · Myong-Ho Jeong[1,3,4] · Jung-Hoon Pyun[1,3] · Hyeon-Ju Jeong[1,3] · Tuan Anh Vuong[1,3,5] · Ju-Hyeon Bae[1,3] · Subin An[1,3] · Su Woo Kim[1,3] · Yong Kee Kim[6] · Dongryeol Ryu[1] · Hyun-Ji Kim[2,3] · Hana Cho[2,3] · Gyu-Un Bae[6] · Jong-Sun Kang[1,3]

Received: 10 August 2021 / Revised: 22 November 2021 / Accepted: 14 December 2021 / Published online: 28 January 2022

Abstract

Angiotensin II (AngII) has potent cardiac hypertrophic effects mediated through activation of hypertrophic signaling like Wnt/β-Catenin signaling. In the current study, we examined the role of protein arginine methyltransferase 7 (PRMT7) in cardiac function. PRMT7 was greatly decreased in hypertrophic hearts chronically infused with AngII and cardiomyocytes treated with AngII. PRMT7 depletion in rat cardiomyocytes resulted in hypertrophic responses. Consistently, mice lacking PRMT7 exhibited the cardiac hypertrophy and fibrosis. PRMT7 overexpression abrogated the cellular hypertrophy elicited by AngII, while PRMT7 depletion exacerbated the hypertrophic response caused by AngII. Similar with AngII treatment, the cardiac transcriptome analysis of PRMT7-deficient hearts revealed the alteration in gene expression profile related to Wnt signaling pathway. Inhibition of PRMT7 by gene deletion or an inhibitor treatment enhanced the activity of β-catenin. PRMT7 deficiency decreases symmetric dimethylation of β-catenin. Mechanistic studies reveal that methylation of arginine residue 93 in β-catenin decreases the activity of β-catenin. Taken together, our data suggest that PRMT7 is important for normal cardiac function through suppression of β-catenin activity.

Keywords PRMT7 · Cardiomyopathy · Wnt · β-catenin

Introduction

Upon stress or pathological signals, cardiac cells undergo remodeling processes associated with myocardial fibrosis and hypertrophy which is one of the major risk factors for heart failure [1]. In cardiac remodeling, the heart reactivates several signaling pathways that are generally active in the developing heart [2]. Accumulating evidence suggests a prominent role of Wnt/β-Catenin (referred to as Wnt signaling hereafter) signaling in cardiac hypertrophy and myocardial fibrosis. The significance of Wnt signaling in cardiomyopathy is underscored by the fact that cardiac remodeling, post-infarct mortality, and cardiac function decline are suppressed by inhibition of Wnt signaling [2]. Chronic infusion of a powerful hypertrophic agent Angiotensin II (Ang II) deregulates Wnt signaling and its suppression is critical for normal cardiac remodeling [3, 4]. Furthermore, deregulated Wnt signaling evokes a progressive dilated cardiomyopathy [5]. Wnt signaling is regulated at multiple levels via complex mechanisms [6]. Upon binding of Wnt ligands to frizzled receptor and co-receptor lipoprotein receptor-related

Byeong-Yun Ahn, Myong-Ho Jeong have contributed equally to this work.

✉ Gyu-Un Bae
gbae@sookmyung.ac.kr

✉ Jong-Sun Kang
kangj01@skku.edu

1 Department of Molecular Cell Biology, Sungkyunkwan University School of Medicine, 2066, Seobu-Ro, Jangan-gu, Suwon 16419, Gyeonggi-do, Republic of Korea

2 Department of Physiology, Sungkyunkwan University School of Medicine, Suwon, Republic of Korea

3 Single Cell Network Research Center, Sungkyunkwan University School of Medicine, Suwon, Republic of Korea

4 Division of Cardiovascular Diseases, Center for Biomedical Sciences, National Institute of Health, Cheongju, Chungbuk, Republic of Korea

5 Research Institute of Aging-Related Disease, AniMusCure, Inc., Suwon, Republic of Korea

6 Drug Information Research Institute, College of Pharmacy, Sookmyung Women's University, 100 Cheongpa-ro 47-gil, Seoul 04310, Republic of Korea

protein (LRP) 5/6, a signaling cascade is initiated to activate β-Catenin by suppression of inhibitory phosphorylation, ubiquitination, and proteosomal degradation, resulting in stabilization and subsequent nuclear translocation of β-Catenin and induction of target gene expression [7]. Recent studies have revealed novel posttranslational modifications that enhance β-Catenin activities. In response to the mechanical or oxidative stress, the tyrosine phosphorylation of β-Catenin by Src family non-receptor tyrosine kinases or acetylation by CBP or p300 can upregulate β-Catenin activities through interaction with transcriptional cofactor TCF [8]. Although the precise modulation of β-Catenin activities appear to be critical for normal cardiac remodeling, the mechanisms of β-Catenin suppression are currently unclear.

Protein arginine methyltransferases (PRMTs) methylate both histone and non-histone substrates on arginine residues, thereby regulating signaling pathways and/or gene expression [9, 10]. Type I PRMTs (PRMT1, 2, 3, 4, 6, and 8) catalyze asymmetric dimethylation while type II PRMTs (PRMT5 and 9) generate symmetric dimethylation of substrates. PRMT7 belongs to the type III enzyme catalyzing monomethylation. PRMT7 is implicated in biological processes, such as proliferation of renal cell carcinomas through regulation of β-Catenin activity [11]. Recent studies with PRMT7 knockout mouse models have uncovered essential roles of PRMT7 in skeletal muscle maintenance and oxidative muscle metabolism associated with aging-related obesity [12, 13]. Furthermore, mutations in the human PRMT7 gene are implicated in recessive disorders such as obesity, digit malformation, and intellectual disability [14, 15]. Recent two studies have reported the physiological importance of PRMT1 in cardiac function using PRMT1 knockout mouse models. PRMT1 deletion in cardiomyocytes caused rapidly progressing dilated cardiomyopathy with heart failure [16, 17]. However, the physiological roles of other PRMTs in cardiac function remains unclear.

In our previous study [12], PRMT7 knockout mice exhibited aging-related obesity that might affect cardiac function. In the pilot study, we have observed that PRMT7 knockout mice exhibited the exercise intolerance phenotype, likely associated cardiac function. Based on these facts, we hypothesized the important role of PRMT7 in the control of cardiac function. Therefore, we investigated the roles of PRMT7 in cardiac function using mouse models lacking PRMT7 in whole body or in cardiomyocytes. PRMT7 expression was downregulated in hypertrophied hearts by chronic Ang II infusion. The deletion of PRMT7 in cardiomyocytes in vivo and in vitro caused cardiac hypertrophy and fibrosis. Cardiac-specific PRMT7 deletion exacerbated Ang II-triggered cardiac hypertrophy. Cardiac transcriptome study of PRMT7-deleted hearts showed the alteration in gene expression profile related to Wnt signaling pathway. Consistently, the open database analysis related to Ang II-cardiac hypertrophy revealed the inverse correlation between PRMT7 and Wnt signaling genes. Mechanistic studies revealed that PRMT7 suppresses Wnt signaling pathway by methylation of β-Catenin at arginine residue 93, which is critical for the regulation of β-Catenin activity in the control of cardiac hypertrophy and fibrosis.

Materials and methods

Mice experiments

PRMT7$^{\pm}$ mice were maintained as previously described [12]. Briefly, PRMT7$^{<tm1a(EUCOMM)wtsi>}$ mice purchased from Sanger Institute were backcrossed onto C57BL/6 J background for at least 10 generations. Littermate wildtype mice were used for control groups of PRMT7$^{-/-}$ mice in all experiments. For generation of cardiac-specific PRMT7 null mice, PRMT7$^{Tm1c/Tm1c}$ (PRMT7$^{f/f}$) mice were crossed with mice carrying Myh6-Cre transgene (Jackson Laboratory; Tg(Myh6-cre)2182Mds/J). Genotyping was performed as previously described [12]. To assess the effect of PRMT7 in cardiomyopathy, these studies used about 4 months-old littermate male mice from heterozygous breeding. For development of cardiac hypertrophy, 10 weeks-old mice were treated with angiotensin II (Ang II). Mice were infused with Ang II (1.5 mg/kg/day) by subcutaneous implantation of osmotic minipump (Alzet model 1002) for 14 days [18, 19].

For echocardiographic analysis, mice were anesthetized with 1–2% (vol/vol) isoflurane. Echocardiography was performed at 4 months-old mice and 1 day before sacrifice, using a Vevo LAZR-X photoacoustic imaging system (Fujifilm visual sonics). Heart rates are monitored and generally maintained at 400–500 beats per minute. Analyses of M-mode images derived from the short-axis view of left ventricle (LV) was performed to calculate ejection fraction (EF) and fractional shortening (FS).

For animal studies, drug infusion and injection were approved by the Institutional Animal Care and Use Committee (IACUC) of Sungkyunkwan University School of Medicine (SUSM) and carried out by the ethical guideline (the protocol number: SKKUIACUC 2020-04-14-1).

Cell cultures, transfection and reporter assays

HEK293T, 10T1/2 and H9c2 cells were cultured in Dulbecco's Modified Eagle's Medium (Gibco) containing 10% fetal bovine serum (Gibco) and 1% penicillin/streptomycin. Transfection studies were performed as previously described [20]. Lipofectamine 2000 (Invitrogen) was used for 10T1/2 cells, while polyethylenimine (1 mg/ml, Sigma-Aldrich) was used for H9c2 cells. To assess the effects of PRMT7 inhibition of Wnt signaling, cells were treated with 50 μM DS437,

a dual inhibitor for PRMT5 and PRMT7 (Sigma-Aldrich) in combination with 0.2% BSA or 20 ng/ml Wnt3a (R&D systems). To inhibit Wnt signaling activity, 4 μM XAV939 (Calbiochem) was used.

To isolate primary cardiomyocytes, 5 months-old PRMT7$^{+/+}$ and PRMT7$^{-/-}$ littermates were used. Both ventricular and atrial myocytes were isolated by perfusion with a Ca^{2+}-free normal Tyrode solution containing collagenase (Worthington Type 2) on a Langendorff column at 37 ºC, as previously described [21]. Neonatal rat ventricular myocyte (NRVM) cells were isolated from neonatal Sprague–Dawley (SD, 1–2 days) rat heart tissues as previously described [16]. To induce cellular hypertrophy, the cell culture medium was replaced with serum-free culture medium for 48 h with angiotensin II (Ang II, 1 μM, Sigma-Aldrich).

Luciferase reporter assay was performed as previously described [22]. Briefly, 10T1/2 and H9c2 cells were transfected with 0.7 μg of control or PRMT7 overexpression plasmids, 0.3 μg of β-Catenin-responsive Top-Flash luciferase construct and 0.1 μg of β-galactosidase plasmid of ratio for 1.1 μg of total DNA. Twenty-four hours after transfection, cells were analyzed for luciferase activity, according to manufactures protocol (Promega). To further analyze the transcriptional activity of control WT and mutant β-Catenin, TCF/LEF;H2B-GFP reporter plasmid construct (Addgene, Plasmid #32,610) was co-transfected with control or mutant β-Catenin constructs into 10T1/2 cells. The GFP-positive 10T1/2 cells were counted with TissueFAXS PLUS (TISSUEGNOSTICS) and images were analyzed with TissueQuest image analysis software.

Protein, mass spectrometry and RNA analysis

Immunoblotting and immunostaining were performed by previously described [23]. To examine the protein interaction between PRMT7 and β-Catenin, 1 mg of lysates and 1 μg of primary antibodies were used. Samples were immunoprecipitated with 20 μg of dynabeads-Protein A or Protein G (Invitrogen). The density of immunoblotting bands was measured by Image J with independent triplicates. To analyze posttranslational modification of β-Catenin protein, 1 mg of sample lysates were immunoprecipitated with 1 μg of anti-β-Catenin and anti-Flag antibodies. The primary antibodies used in this study were listed in Supplementary Table S1.

In vitro methylation assay was performed as previously described [24]. Two mg recombinant GST-β-Catenin (Sigma-Aldrich) were incubated with beads bound to PRMT7-HA or inactive form of PRMT7-HA (iP7) and 50 mM S-(5'adnosyl)-L-methionine chloride dihydrochloride (SAM) (Sigma-Aldrich, St. Louis, MO) in reaction buffer (20 mM Tris–HCl, pH 8.0, 200 mM NaCl, 0.4 mM EDTA) for 1 h at 37 ºC. Reaction samples were subjected to SDS-PAGE and Western blot with anti-Sym10 and MMA antibodies to analyze the methylation status.

For mass spectrometry, Flag-tagged β-Catenin was transfected into HEK293T cells and β-Catenin proteins were immunoprecipitated using Flag antibodies. Mass spectrometry analysis of purified Flag-β-Catenin protein was performed by Medicinal Bioconvergence Research Center, Seoul National University. Mass spectrometry was carried out as described.

Quantitative RT-PCR was performed as previously described [25]. Total RNAs from mouse hearts and NRVM cells were extracted with easy-BLUE (iNtRON) reagent following the manufacturer's instructions. cDNA samples were generated from 0.5 μg of RNAs with PrimeScript RT reagent kit (TaKaRa) according to manufactures' protocol. The primer sequence used in this study are listed in Supplementary Table S2. High-throughput sequencing was performed as single-end 75 sequencing using Illumina NExtSEq 500 (ebiogen, Korea). The analysis for RNA sequencing data was performed using ExDEGA v3.0 (ebiogen) and heatmap was displayed utilizing Morpheus (http://software.broadinstitute.org/morpheus/). The global gene expression was assessed by the reactome with Gene Set Enrichment Analysis (GSEA) (http://www.gsea-msigdb.orb/gsea/msigdb/index.jsp) using MsigDB database v7.2 (> 1.3 fold, RC $\log2 > 2$, $p < 0.05$).

Histology and immunofluorescence

Histology of heart sections was performed as previously described [21, 26]. Briefly, harvested mouse hearts were fixed with 4% paraformaldehyde (PFA) and embedded into paraffin block or optimal cutting temperature (OCT, Sakura Finetec). Praffin-embedded heart samples were sectioned at the 5–7 μm thickness and then stained with hematoxylin and eosin stain (BBC biochemical), Masson's trichrome, or Sirius Red staining (Abcam). Immunohistochemistry of PRMT7 in heart samples was performed as described previously [21]. Immunofluorescence was performed as previously described [27]. Briefly, cells were grown on coverslips and transfected with control and pcDNA-HA-PRMT7 or pSuper shPRMT7 to overexpress or deplete PRMT7. In addition, to analyze the effects of PRMT7 on cardiomyocyte hypertrophy, cardiomyocytes were transfected with an inactive form of PRMT7 (iPRMT7) harboring two mutant residues (E144A and E478A) in the catalytic domain. Cells were then fixed with 4% PFA and permeabilized with 0.2% Triton X-100 in PBS, followed by blocking (2% BSA or 5% goat serum in PBS). Primary and secondary antibodies were diluted with blocking solution and incubated overnight at 4 ºC or 1 h at room temperature. Fluorescence images were analyzed with an LSM-710 confocal microscope system (Carl Zeiss) and Nikon ECLIPSE TE-2000U, as previously described [28]. For quantification of the surface area of

primary cardiomyocytes and NRVM cells was analyzed by NIS-Elements F software (Nikon) and Zen 3.1 Blue (Zeiss). To label the primary cardiomyocytes in culture, cells were pseudo-colored, followed by cell size quantification.

Site directed mutagenesis

To generate the point mutations of R93A and R591A of β-Catenin, site-directed mutagenesis was performed with QuickChange II XL Site-Directed Mutagenesis Kit (Agilent) followed by manufacture's protocol. In brief, mutant β-Catenin plasmids were synthesized with 0.5 μg of the template (pcDNA-Flag-human β-Catenin) in the sample reaction buffer. After the sample reaction, 1 μg of Dpn1 restriction enzyme was immediately incubated at 37 ºC for 1 h to digest the parental supercoiled dsDNA and transformed into DH5α competent cells. The primer sequences for mutagenesis are described in Supplementary Table S3.

Bioinformatics analysis

The cardiac transcriptomes of all available organisms (112 datasets) from the NCBI Gene Expression Omnibus (GEO; http://www.ncbi.nlm.nih.gov/geo) database were computed for Pearson's correlations between *PRMT7* and each gene belong to the gene set of the Wnt signaling pathway (*Ctnnb1*, *Axin2*, *Gsk3b*, and *Isl1*) with the Graphpad PRISM7. Heatmap was visualized using Morpheus (http://www.software.broadinstitute.org/morpheus/) followed by hierarchical clustering (One-minus Pearson's coefficient).

Statistical analysis

Values are means ± SEM or SD as noted. Statistical significance was calculated by paired or unpaired two-tailed Student's *t*-test or Analysis of variance (ANOVA) test followed by Tukey's test; differences were considered significant at $p < 0.05$.

Results

PRMT7 is declined in cardiac hypertrophy evoked by chronic Ang II treatment

To characterize the role of PRMT7 in cardiac function, the immunostaining against PRMT7 in human and mouse hearts were examined for the expression of PRMT7. Immunostaining result displayed that PRMT7 is expressed in cardiomyocytes (Fig. S1a, b). For analyzing the subcellular location of PRMT7 in cardiomyocytes, immunostaining against PRMT7 with α-Actinin in neonatal rat ventricular cardiomyocytes (NRVMs) revealed that PRMT7 was located on the nucleus as well as the cytosol (Fig. S1c). Next, we have analyzed the datasets (GDS4310, GDS3661, GDS3684, GDS3228 and GDS3465) obtained from mouse hearts with cardiomyopathies (CP) induced by surgery and drug: Angiotensin II (GDS4310), spontaneous heart failure (GDS3661), Isoproterenol (GDS3684), aortic band (GDS3228), and transverse aortic constriction (GDS3465). The expression of *Prmt7* was significantly reduced in disease models, implicating the potential involvement of PRMT7 in cardiac function (Fig. 1a). To understand the role of PRMT7 in cardiac function, the expression pattern of PRMT7 was examined in cardiac hypertrophy. As previously reported [4], the chronic treatment of angiotensin II (Ang II) for 2 weeks elicited cardiac hypertrophy and myocardial fibrosis (Fig. 1b, c). Consistently, the expressions of myocardial fibrosis genes such as Atrial Natriuretic Peptide (ANP) and Collagen 1α1 (COL1A1) were elevated, while PRMT7 proteins were greatly reduced in hearts infused with Ang II for 2 weeks, relative to control hearts (Fig. 1d). To further assess the effects of cardiac hypertrophy on PRMT7 expression, NRVMs were treated with Ang II for 3 days. Similar to the in vivo effect, Ang II treatment decreased PRMT7 proteins, while elevated ANP and COL1A1, compared to the control (Fig. 1e). Collectively, these data suggest that PRMT7 might play the pivotal role in cardiac function.

PRMT7 deletion in cardiomyocytes induces cardiac hypertrophy

To examine the effect of acute PRMT7 depletion in cardiomyocytes, NRVM cells transfected with 2 different PRMT7 shRNAs. PRMT7 proteins were decreased by tested shRNAs with variable efficiencies (Fig. 2a). PRMT7 depletion by shRNA#1 in NRVM cells evoked hypertrophic responses, as seen in about twofold enlargement of cell surface area (Fig. 2b, c). The capacitance analysis confirmed this increased size of PRMT7-depleted NRVMs (Fig. S2a). Furthermore, the expression of fibrotic response genes, ANP, Brain Natriuretic Peptide (BNP), and β-Myosin Heavy Chain (β-MHC) was significantly elevated in PRMT7-depleted NRVM cells with shRNA#1 or 2, compared to control shRNA-transfected cells (Fig. 2d). In addition, $PRMT7^{+/+}$ (WT) and $PRMT7^{-/-}$ (KO) cardiomyocytes were isolated from hearts and subjected to analysis for cell size and capacitance. PRMT7-deficient cardiomyocytes were morphologically enlarged, compared to wildtype cardiomyocytes (Fig. S2b, c). Also, the capacitance analysis revealed a dramatically increased size of KO atrial and ventricular cardiomyocytes, compared to wildtype cells (Fig. S2d). In addition, the hematoxylin and eosin (H&E) staining showed cardiac hypertrophy in KO hearts and the fibrosis staining revealed increased fibrotic area around enlarged cardiomyocytes (Fig. 2e, f). Furthermore, PRMT7-deficient hearts exhibited

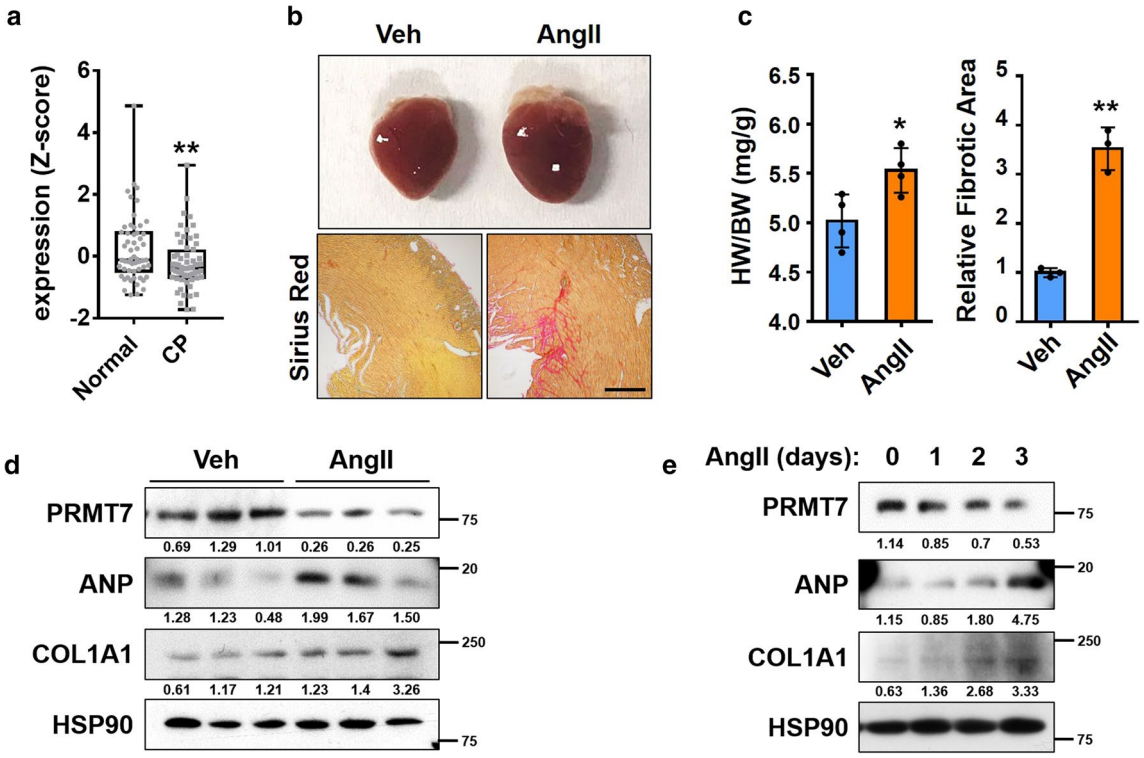

Fig. 1 PRMT7 is decreased in cardiac hypertrophy induced by chronic Ang II treatment. **a** Boxplot showing the expression of *Prmt7* in hearts from normal conditions ($n=58$) and cardiomyopathy models (CP) ($n=63$) (GSE4310, GSE3661, GSE3684, and GSE3981). **b** Representative images for a photograph and Sirius Red staining of hearts infused with angiotensin II (Ang II) for 2 weeks. Scale bar: 100 μm (Lower). **c** The relative heart weight of Ang II-infused mice normalized by the body weight. $n=4$ per each group. $^{*}p<0.05$. Data represent ± SD (Left). Quantification of the fibrotic area in whole heart areas ($n=3$) as shown in panel (**b**). $^{**}p<0.01$. Data represent ± SEM (Right). **d** Immunoblot analysis of hearts administrated with Ang II. (**e**) Immunoblot analysis of neonatal rat ventricular cardiomyocytes (NRVMs) cultured with Ang II for 3 days

substantially increased levels of ANP and COL1A1, markers for hypertrophy and fibrosis (Fig. 2g). However, the expression of other PRMTs including PRMT1, PRMT4, and PRMT5 was not significantly altered. These data suggest that PRMT7 deficiency causes cardiomyocyte hypertrophy.

PRMT7 deficiency exacerbates the Ang II-induced cardiomyopathy

Next, we examined the effect of PRMT7 deficiency in Ang II-induced cardiomyopathy using cardiac-specific PRMT7-deleted mice. We have generated mice lacking cardiomyocyte-specific PRMT7 by breeding $PRMT7^{Tm1C/Tm1c}$ ($PRMT7^{f/f}$, WT) mice with $PRMT7^{f/f}$ mice carrying a single copy of cardiac-specific myosin-heavy chain (Myh6)-Cre recombinase. Resulting littermates of $PRMT7^{f/f}$ and $PRMT7^{f/f;Myh6-cre}$ (cKO) were born in the ratio of 53.7–46.3%, respectively. Vehicle or Ang II-infused WT and cKO mice for 2 weeks were examined by echocardiographic analysis. Chronic Ang II infusion impaired cardiac function with decreased the ejection fraction (EF) and the fractional shortening (FS) in both WT and cKO mice, however PRMT7 deficiency exacerbated cardiac dysfunction caused by Ang II (Fig. 3a, b). In addition, PRMT7 deficiency aggravated Ang II-induced cardiac hypertrophy and myocardial fibrosis (Fig. 3c–e). Consistently, the protein level of ANP was markedly elevated in Ang II-infused WT and cKO hearts (Fig. 3f). Taken together, these data suggest that PRMT7 might play a protective role against cardiomyopathy triggered by Ang II.

PRMT7 overexpression attenuates Ang II-induced cardiomyocyte hypertrophy

Next, we have examined the protective effects of PRMT7 overexpression on cardiomyocyte hypertrophy. NRVM cells were transfected with control pcDNA or HA-tagged PRMT7 (PRMT7-HA), followed by the treatment with Ang II. In contrast to the hypertrophic response caused by PRMT7 depletion, PRMT7 overexpression attenuated ANP induction triggered by Ang II treatment (Fig. 4a). Additionally, PRMT7-overexpressing cardiomyocytes exhibited smaller cell size in both vehicle and Ang II treatment, compared to control-transfected cells (Fig. 4b, c). Taken together, these

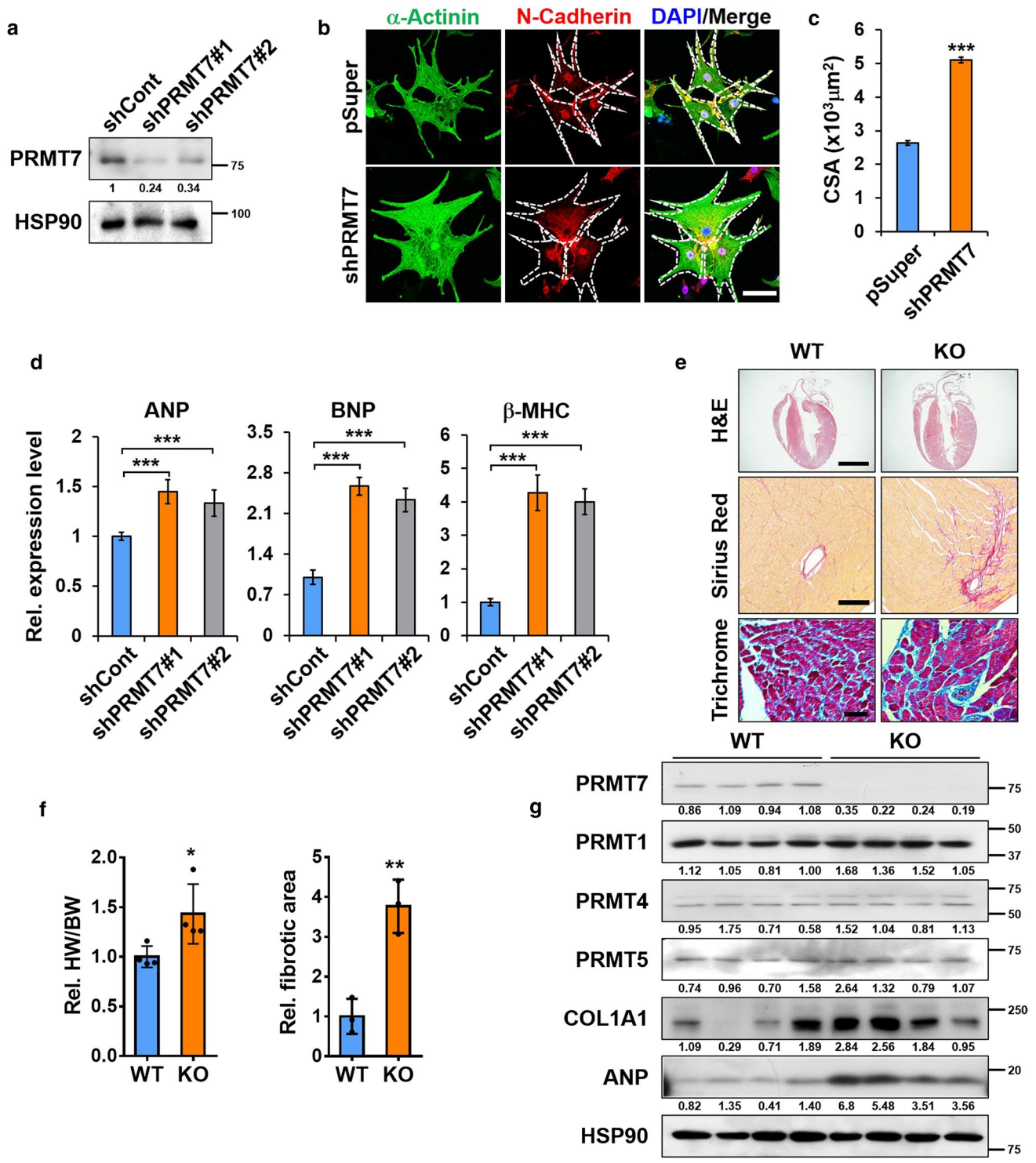

Fig. 2 PRMT7 deficiency impairs cardiac function with cardiac hypertrophy and fibrosis. **a** Immunoblot analysis for PRMT7 depletion in neonatal rat ventricular cardiomyocyte (NRVM) cells. **b** Representative immunostaining images of control or shPRMT7-expressing NRVM cells. The white dashed line indicates the cellular boundary. Scale bar: 50 μm. **c** Quantification of the cell surface area in experiments similar as shown in the panel (**b**). n = 76 for pSuper, and $n = 60$ for shPRMT7. $^{***}p < 0.005$. Data represent ± SEM. **d** qRT-PCR analysis for cardiac hypertrophy markers. $n = 3$, $^{***}p < 0.005$. Data represent ± SE. **e** Representative images for hematoxylin and eosin (H&E), Sirius Red, and Masson's Trichrome staining of WT and KO hearts. Scale bar: 500 μm (Upper) and 100 μm (Middle and Lower). **f** The relative heart weight of WT and KO normalized by the body weight. $n = 4$ per each group. $^{*}p < 0.05$. Data represent ± SD (Left). Quantification of the fibrotic area in whole heart areas ($n = 3$) as shown in panel (**e**). $^{**}p < 0.01$. Data represent ± SEM (Right). **g** Immunoblot analysis of WT and KO hearts

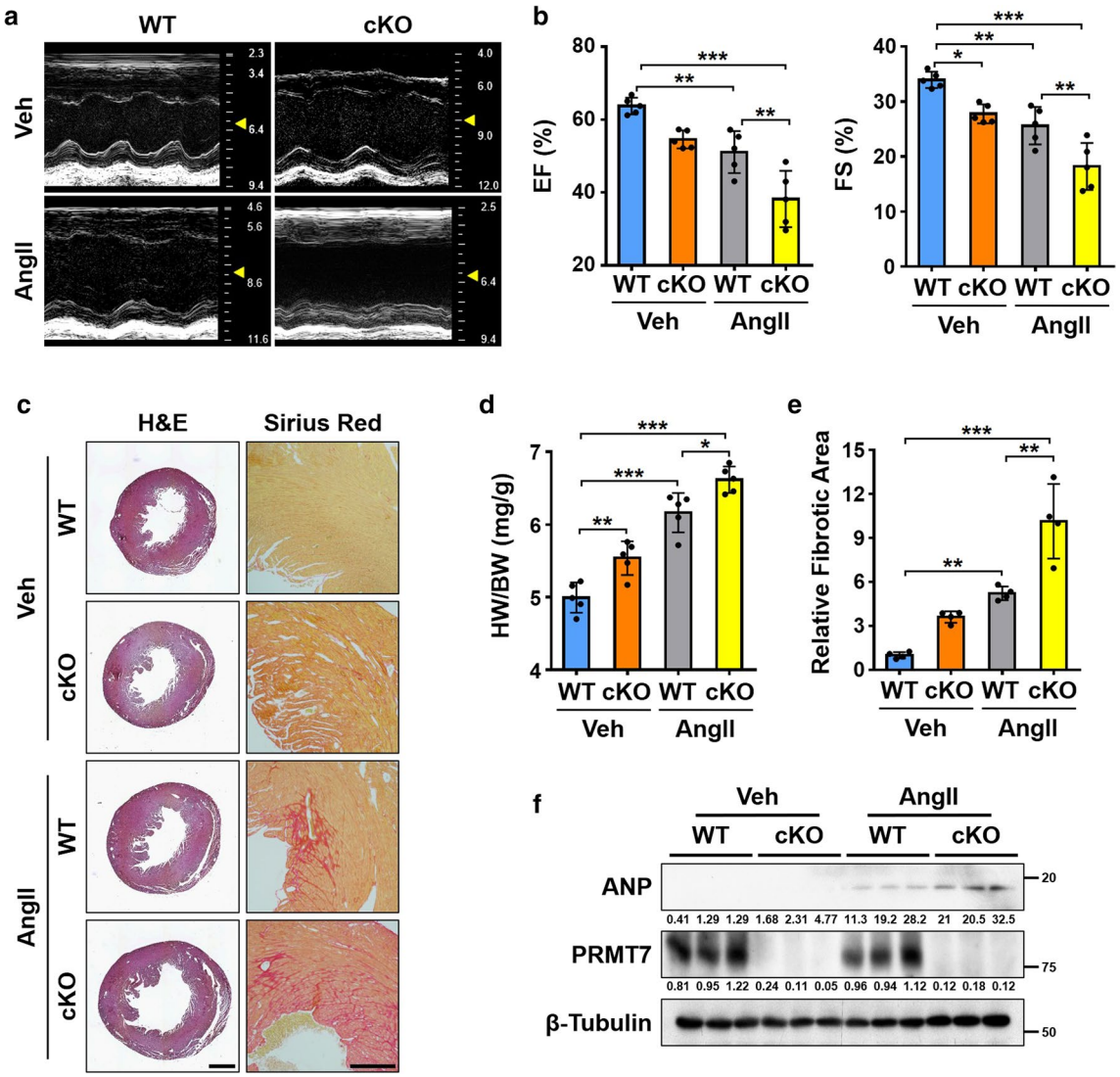

Fig. 3 PRMT7 deficiency exacerbates Ang II infusion cardiomyopathy. **a** Representative echocardiographic images of WT and cKO infused with vehicle (Veh) or angiotensin II (Ang II). **b** Echocardiographic parameters of WT and cKO infused with Veh or Ang II. *EF* the ejection fraction, and *FS* the fractional shortening. $n=5$, $^{*}p<0.05$, $^{**}p<0.01$, $^{***}p<0.005$, one-way ANOVA. Data represent ± SEM. **c** Representative images for hematoxylin and eosin (H&E) stain and Sirius Red stain of WT and cKO infused with Ang II. Scale bar: 1 mm (Left) and 100 μm (Right). **d** The relative heart weight of WT and cKO mice infused with Ang II. $n=5$ per each group. $^{*}p<0.05$, $^{**}p<0.01$, $^{***}p<0.005$, one-way ANOVA. Data represent ± SD. **e** Quantification of the fibrotic area in whole heart areas ($n=4$) as shown in panel (**c**). $^{**}p<0.01$, $^{***}p<0.005$, one-way ANOVA. Data represent ± SEM. **f** Immunoblot analysis of WT and cKO hearts infused with Ang II

data suggest that PRMT7 suppresses cardiomyocyte hypertrophy elicited by Ang II.

PRMT7-deficient hearts exhibit the alteration in gene expression profile related to Wnt signaling

To investigate the molecular mechanisms of PRMT7 in cardiac hypertrophy, we performed RNA sequencing with WT and KO hearts followed by the Kyoto Encyclopedia of Genes and Genomes (KEGG) pathway analysis (> 1.3 fold, an average of normalized RC log2 > 2, p value < 0.05). The RNA sequencing data revealed that KO hearts had 450 downregulated and 489 upregulated genes, compared to the WT hearts (Fig. 5a). Genes involved in pathways related to Wnt, TLR, and JAK/STAT signaling were altered in KO hearts (Fig. 5b). Recent studies reported the implication of Wnt signaling in cardiac hypertrophy and fibrosis [2, 29]. The heatmap analysis shows the alteration in genes related to Wnt signaling in KO hearts (Fig. 5c). To analyze the relationship between PRMT7 and Wnt signaling, we examined 112 sets ($n=1103$) of cardiac transcriptomes from 6 organisms (Homo sapiens,

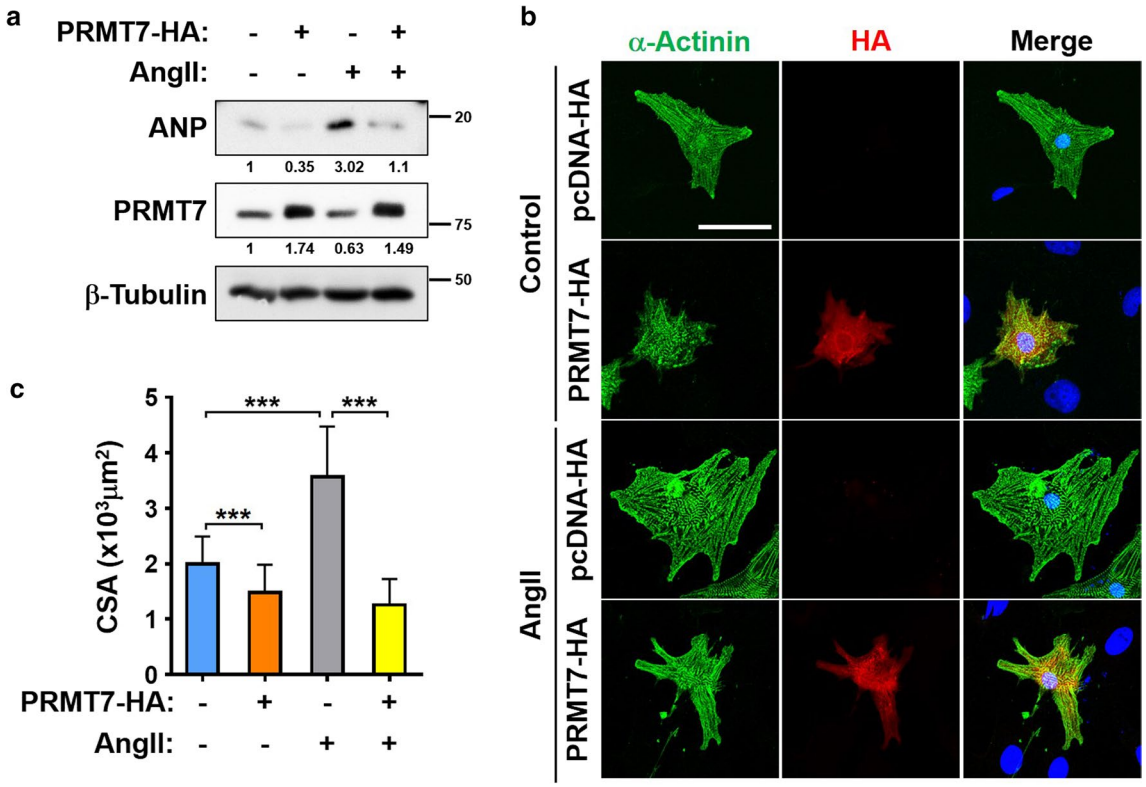

Fig. 4 Ang II-induced cardiac hypertrophy is attenuated by PRMT7 overexpression. **a** Immunoblot analysis for ANP expression in pcDNA or PRMT7-overexpressing NRVM cells cultured with Ang II. **b** Representative immunostaining images of NRVM cells expressing PRMT7-HA treated with Ang II for 48 h. HA (red) and α-Actinin (green). Scale bar: 20 μm. **c** Quantification of the cell surface area in experiments similar as shown in panel (**b**). $n=70$ (pcDNA-HA + control); $n=56$ (PRMT7-HA + control); $n=57$ (pcDNA-HA + Ang II); $n=53$ (PRMT7-HA + Ang II). $^{***}p<0.005$, one-way ANOVA. Data represent mean ± SEM

Mus musculus, Rattus norvegicus, Canis lupus, Sus scrofa, and Danio rerio) as an unbiased survey (Fig. S3a). We found an inverse correlation between *PRMT7* and major Wnt signaling targets, *Ctnnb1*, *Axin2*, and *Isl1* (Fig. S3b). Furthermore, the negative correlation between *Prmt7* and *Ctnnb1* was observed in 4 different species (Homo sapiens, Mus musculus, Canis lupus, and Danio rerio) (Fig. S3c). In addition, GEO dataset GDS4310 from hypertrophic cardiomyopathies induced by Ang II infusion [30] revealed a negative correlation between *Prmt7* and *Ctnnb1*, the hierarchical cluster analysis divided into two opposing groups (Fig. 5d). *Ctnnb1*, *Axin2*, and *Isl1* were clustered as one group which was separated from the *PRMT7* group. To verify this inverse correlation, we have examined the levels of β-Catenin in hearts infused with Ang II. Ang II-infused hearts displayed downregulated levels of PRMT7, while β-Catenin was increased in Ang II-infused hearts (Fig. 1d and 5e). Consistently, PRMT7-depleted NRVMs and KO hearts exhibited elevated β-Catenin proteins, compared to controls (Fig. 5f, g). Taken together, these data suggest that PRMT7 deficiency activates the Wnt signaling pathway.

PRMT7 suppresses β-Catenin activation

To further assess the relationship between PRMT7 and β-Catenin, NRVM cells were treated with an inhibitor of PRMT7, DS437. DS437 treatment enhanced the level of active β-Catenin (β-Catenin*) and total β-Catenin proteins without affecting Prmt5 or PRMT7 levels (Fig. 6a). Consistently, immunostaining against β-Catenin revealed that NRVMs treated only with DS437 exhibited a significant increase in nuclear β-Catenin accumulation which was further elevated by Wnt3a treatment (Fig. 6b, c). To verify the role of PRMT7 in β-Catenin activation, PRMT7 overexpression in 10T1/2 MEFs attenuated the activity of a Topflash Wnt-reporter, compared to control (Fig. 6d). In a converse experiment, control or PRMT7-depleted NRVM cells were treated with DMSO or a Wnt signaling inhibitor XAV939. PRMT7 depletion in NRVM cells enhanced the expression of Axin2 and ANP, compared to control cells. XAV939 treatment resulted in decreased Axin2 and ANP expression in both control and PRMT7-depleted NRVM cells. However, the expression of Axin2 and ANP was still higher in PRMT7-depleted NRVM cells (Fig. 6e). To further assess,

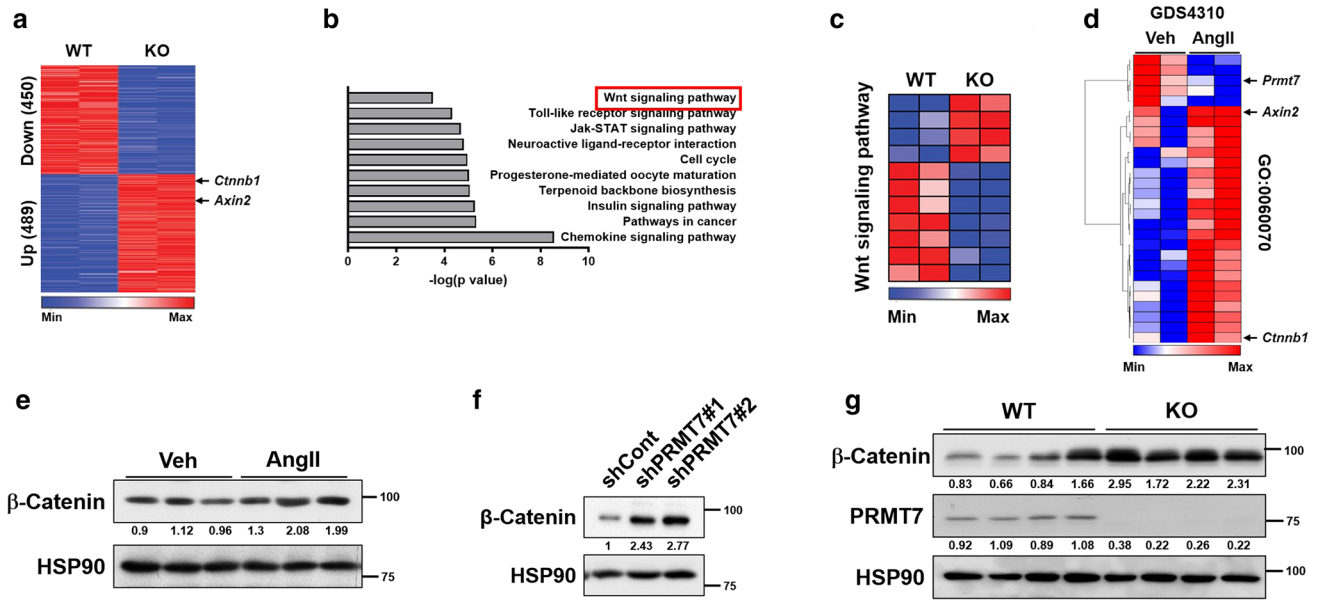

Fig. 5 PRMT7-deficient hearts show altered gene expression profiles related to Wnt signaling. **a**, **b** Comparision of Gene Set Enrichment Analysis for reactome database clusters of genes up- and downregulated between WT and KO hearts ($n=2$, with biological repeat, >1.3 fold, normalized with RC $\log2>2$, $p<0.05$). **c** The heatmap for RNA expression involved in Wnt signaling pathway-related genes. **d** The heatmap showing gene expression patterns of the canonical Wnt signaling pathway (GO:0060070) in either Vehicle- or Ang II-treated cardiac transcriptome (GDS4310). **e** Immunoblot analysis for Ang II-infused hearts. **f**, **g** Immunoblot analysis for β-Catenin in PRMT7-depleted NRVM cells and hearts

H9c2 cardiomyocytes were transfected with PRMT7-HA expression vectors and treated with Wnt3a, followed by immunoblot analysis and immunostaining for β-Catenin and HA. PRMT7 overexpression attenuated the accumulation of active and total β-Catenin proteins induced by Wnt3a (Fig. 6f). Wnt3a treatment elicited readily detectable nuclear β-Catenin staining in HA-negative cardiomyocytes, while PRMT7-HA-transfected H9c2 cells showed no or weak staining (Fig. 6g, h). Taken together, these data suggest that PRMT7 suppresses β-Catenin nuclear accumulation and activity.

PRMT7 depletion reduces symmetric arginine methylation of β-Catenin

We then investigated the mechanism by which PRMT7 controls β-Catenin activity. Hereof, a possible interaction between PRMT7 and β-Catenin was examined by immunoprecipitation with control IgG or β-Catenin antibodies in heart lysates. PRMT7 was immunoprecipitated with β-Catenin (Fig. 7a). Next, in vitro methylation assay was performed using GST-β-Catenin protein and the immunoprecipitated wildtype PRMT7 and inactive form of PRMT7 (iP7) in the presence of the methyl group donor, S-adenosyl methionine (SAM). Then the immunoblotting analysis was performed by utilizing the MMA and Sym10 antibodies that recognize the mono-methylated and symmetric methylated arginine residues, respectively. PRMT7 induced the mono- and symmetric arginine demethylation of β-Catenin (Fig. 7b), while iP7 attenuated β-Catenin methylation (Fig. S4). To further assess, we asked whether β-Catenin is methylated in NRVM cardiomyocytes by utilizing the MMA and Sym10 antibodies. Both MMA and Sym10-positive β-Catenin proteins were decreased in NRVM cells by DS437 treatment (Fig. 7c, e). Similarly, the basal MMA and Sym10-positive β-Catenin levels were mildly but significantly reduced in KO hearts which correlated well with the elevated β-Catenin level in the lysates, compared to WT hearts (Fig. 7d, f). These data suggest that PRMT7 might regulate β-Catenin through methylation.

β-Catenin activity is regulated through methylation at arginine residue 93 by PRMT7

As a previous study suggests that arginine residue in RXR and arginine-glycine (RG) motif are favorable targets for PRMT7-mediated methylation [31]. The sequence analysis predicted arginine 93 (R93) and R591 as potential methylation sites by PRMT7 (Fig. 8a). Next, we have performed LC–MS/MS analysis using purified flag-tagged human β-Catenin expressed in 293 T cells that express PRMT7. In agreement with the sequence prediction, peptides containing dimethylated arginine residue 93 (R93) and R591 were detected with over 96% and 92% of peptide identification

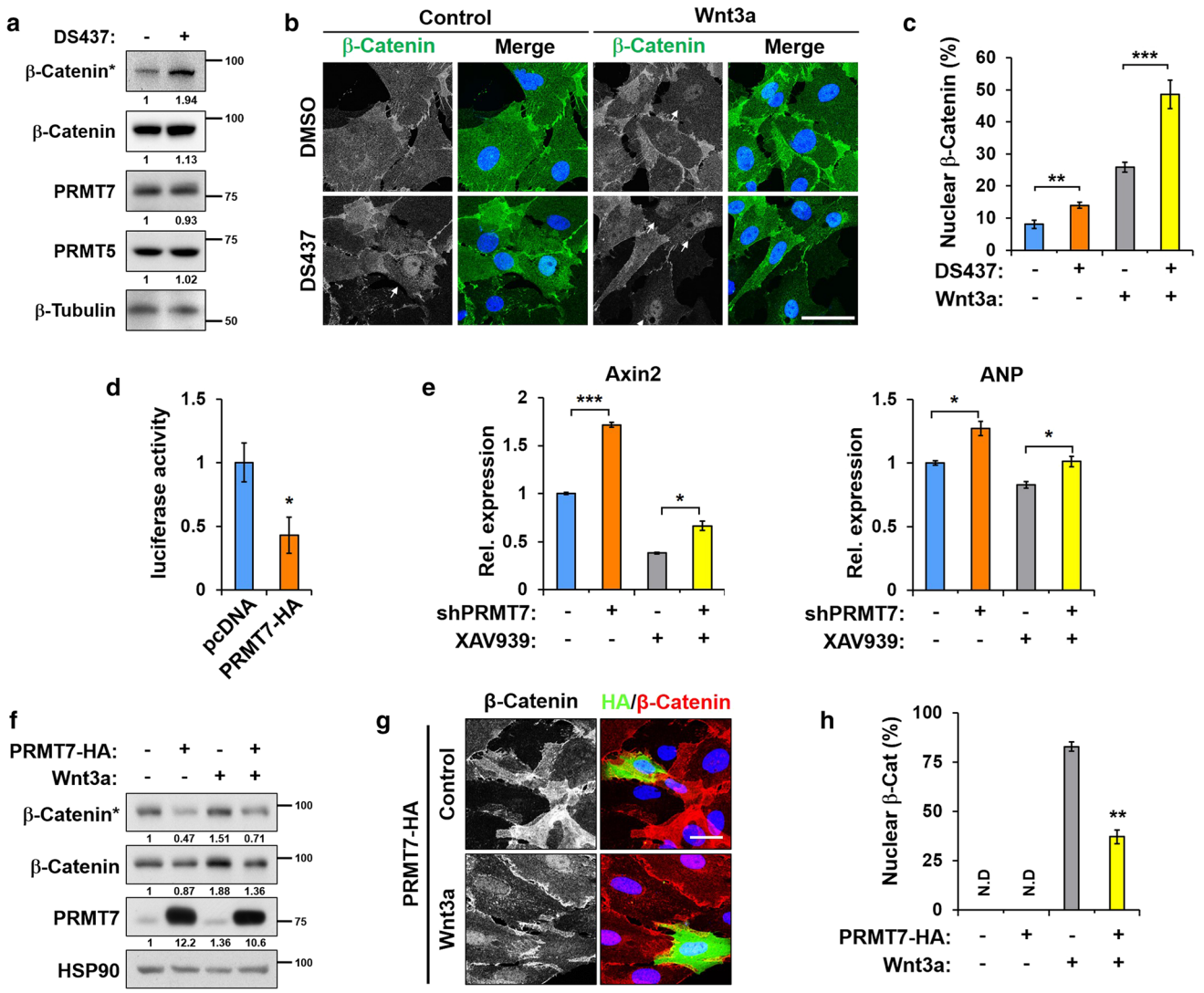

Fig. 6 PRMT7 inactivates the β-Catenin. **a** Immunoblot analysis for active β-Catenin (β-Catenin*) and β-Catenin in NRVM cells cultured with vehicle or DS437, a PRMT7 inhibitor, for 24 h. **b** Representative images of nuclear β-Catenin accumulation in NRVM cells treated with DS437 in response to Wnt3a. Scale bar: 50 μm. **c** Quantification of nuclear β-Catenin accumulation. Mean values of at least 20 fields per each group. $n=3$ per each group, $^{**}p<0.01$, $^{***}p<0.005$. Data represent mean ± SEM. **d** Top-flash luciferase activities in 10T1/2 cells transfected with control or PRMT7. $^{*}p<0.05$, Student's *t*-test. Data represent mean ± SD. **e** Axin2 and ANP expression level in NRVM cells in combination with shPRMT7 and Wnt signaling inhibitor XAV939. $n=3$, $^{*}p<0.05$, $^{***}p<0.005$. Data represent mean ± SD. **f** Immunoblot analysis for β-Catenin expression in control- or PRMT7-overexpressing H9c2 cells in response to Wnt3a. **g** Representative images of nuclear β-Catenin accumulation in PRMT7-overexpressing H9c2 cells cultured with Wnt3a. HA (red), β-Catenin (green) and DAPI (blue). Scale bar: 50 μm. **h** Quantification of β-Catenin accumulation in nucleus. Mean values of at least 20 fields per each group. $n=3$ per each group. *N.D.* not detected, $^{**}p<0.01$. Data represent mean ± SEM

probability, respectively (Fig. 8b). Thus, the arginine-alanine mutants of β-Catenin at R93 and R591 (R93A and R591A; RA) were generated for functional analysis. The symmetric arginine dimethylation (SRM) levels of R93A or R591A mutants were decreased to 40% or 70%, related to WT/β-Catenin, respectively (Fig. 8c, d). Thus, β-Catenin is regulated by methylation at arginine residue 93.

To elucidate whether the methylation of β-Catenin has an effect on its activity, the transcriptional activities of WT/β-Catenin and RA/β-Catenin mutants were analyzed by utilizing the Top-flash luciferase and TCF/LEF;H2B-GFP reporter. The luciferase assay revealed that WT/β-Catenin and R591A mutants augmented comparable levels of luciferase activities, while R93A mutants significant elevated luciferase activities (Fig. 8e). Furthermore, WT/β-Catenin increased H2B-GFP-positive cells, reflecting the level of β-Catenin activity, compared to the control-transfected cells. The R93A mutant further enhanced the percentile of

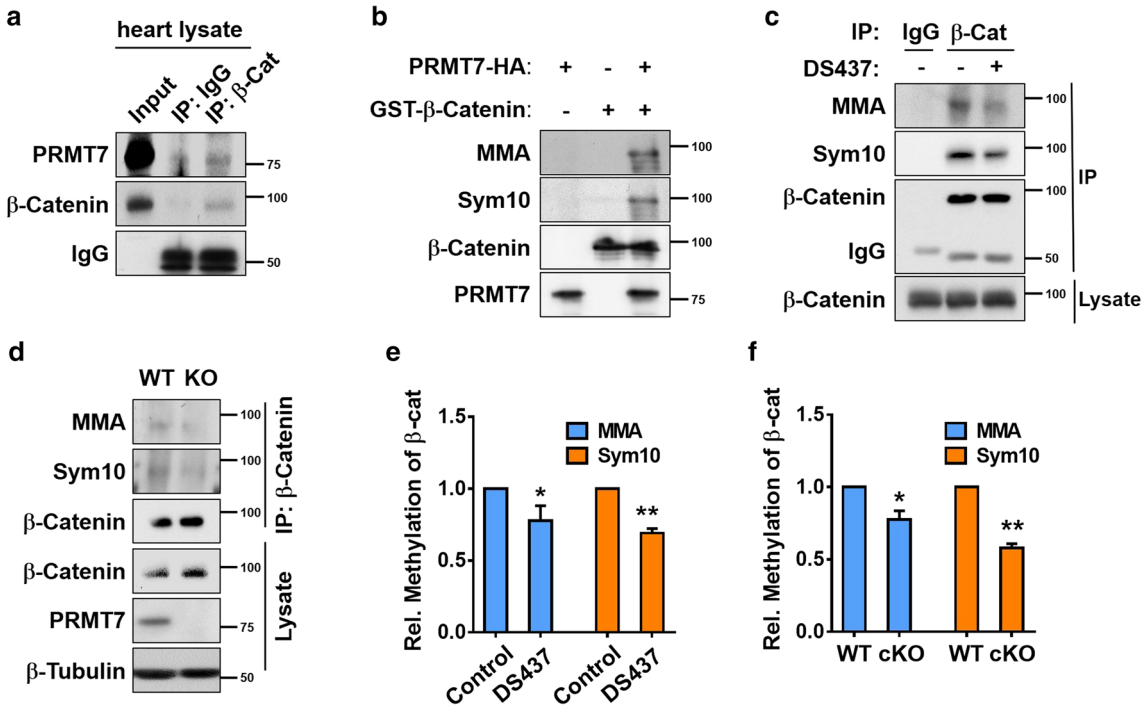

Fig. 7 PRMT7 regulates the arginine methylation of β-Catenin. **a** Co-immunoprecipitation of β-Catenin and PRMT7 in mouse heart lysates. **b** In vitro methylation analysis of recombinant GST-tagged β-Catenin in the presence SAM and purified PRMT7-HA by immunoprecipitation. The methylation status was detected by immunoblotting with anti-MMA and anti-Sym10 antibodies. **c** Arginine monomethylation and symmetric dimethylation of β-Catenin detected by anti-MMA and anti-Sym10 antibodies in NRVM cells cultured with DS437. **d** Immunoblot for mono and symmetric dimethylation of β-Catenin detected in WT and KO hearts. **e**, **f** Quantification of monomethylation and symmetric dimethylation of β-Catenin in NRVM cells treated with DS437 and KO hearts as shown in panel c and d, respectively. $n=3$. $^{*}p<0.05$, $^{**}p<0.01$. Data represent mean ± SD

H2B-GFP-positive cells, while the R591A mutants exhibited a similar activity relative to WT/β-Catenin (Fig. 8f, g). In agreement with these results, H2B-GFP levels were elevated in all forms of β-Catenin expression cells, compared to control cells. WT/β-Catenin and R591A mutant induced similar levels of H2B-GFP proteins, whereas R93A mutant-expressing cells further increased H2B-GFP levels (Fig. 8h). Taken together, these data suggest that PRMT7 negatively regulates β-Catenin activity through methylation at R93.

Discussion

In the current study, we demonstrate the suppressive function of PRMT7 in the cardiac hypertrophic response. A recent proteomic study on protein mutation in cardiomyopathies suggested that mutation at arginine residues is found frequently in cardiomyopathies, implicating the pivotal role of PRMTs in cardiac function [32]. Maladaptive cardiac hypertrophy in disease conditions is accompanied by alterations in the contractile properties with the expression of fetal contractile genes and increased expression of extracellular matrices, such as collagens and fibronectins [33–35]. PRMT7 KO cardiomyocytes and acute depletion of PRMT7 in NRVMs exhibited enlarged cell size and alteration in the expression of fetal genes, likely contributing to the decreased cardiac contractile function of PRMT7 cKO mice infused with Ang II. These data suggest that PRMT7 is critical for normal remodeling of the cardiomyocytes and PRMT7 depletion causes maladaptive cardiac remodeling leading to the cardiac hypertrophy. Interestingly, PRMT7 depletion in cardiomyocytes resulted in nuclear β-Catenin accumulation and target gene expression. These results are in line with the notion that dysregulated Wnt signaling is implicated in maladaptive cardiac remodeling leading to cardiac hypertrophy and fibrosis [36]. Previous studies have demonstrated that the chronic infusion of Ang II deregulates Wnt signaling and its suppression is critical for normal cardiac remodeling [3, 4, 37]. Our current study further supports the importance of Wnt signaling regulation in cardiac hypertrophic response. Our current study revealed an inverse relationship between PRMT7 and β-Catenin expression in PRMT7-depleted cardiomyocytes. This inverse correlation was further supported by the open database correlation studies using 112 data sets. Thus, it is likely that PRMT7 functions as a negative regulator of β-Catenin. Consistently,

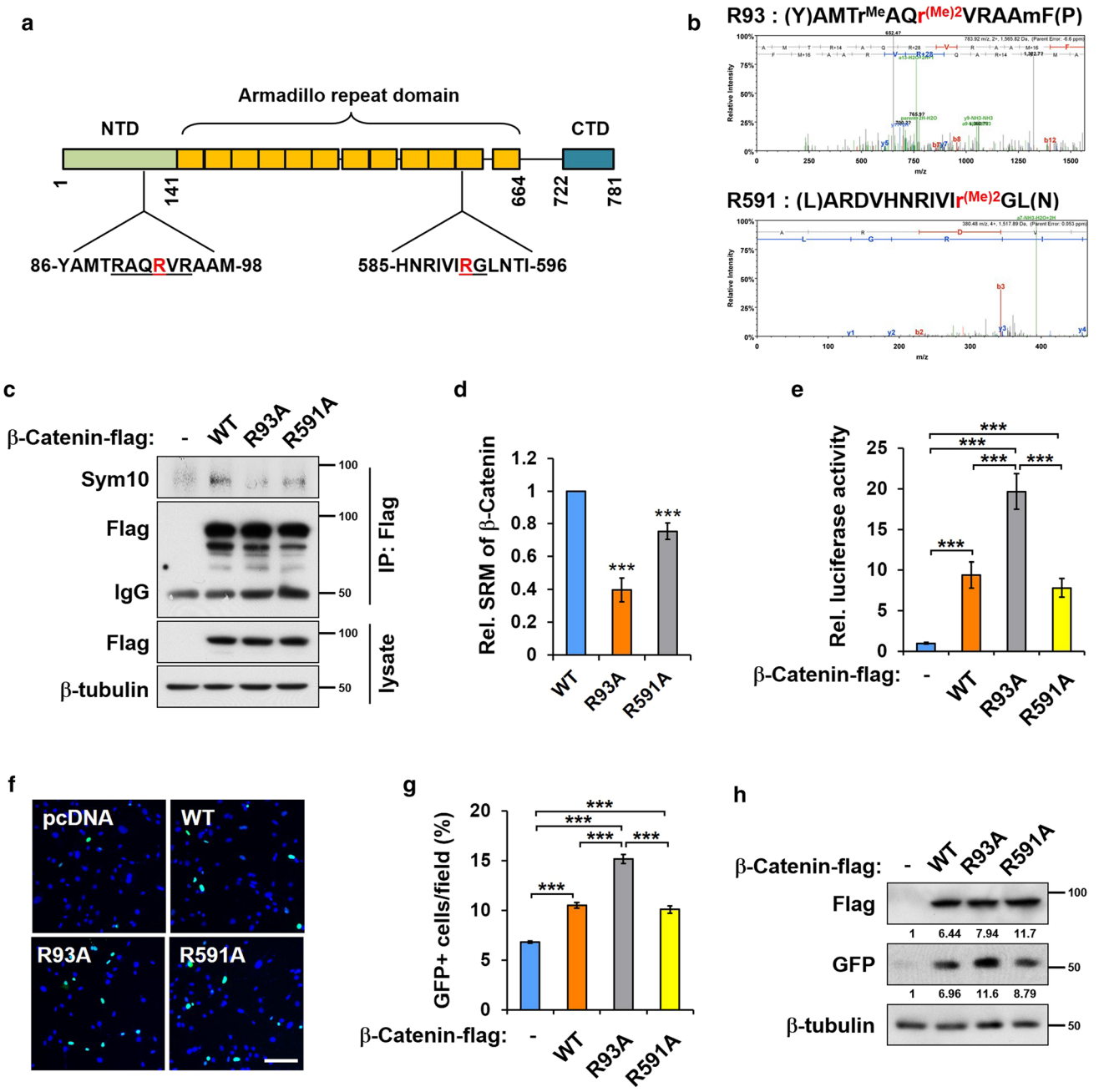

Fig. 8 PRMT7 methylates β-Catenin at arginine residue at 93, regulating the activity of β-Catenin. **a** Schematic representation showing two potential methylation sites predicted by sequence analysis. **b** LC–MS/MS spectrum of human-β-Catenin derived peptides (98% coverage) showing symmetric dimethylation (SRM) sites on arginine 93 (R93; AMTr^{Me}AQr$^{(Me)2}$VRAAmF) with 96% of peptide identification probability and R591 (ARDVHN-RIVIr$^{(Me)2}$GL) with 92% of peptide identification probability. **c** Immunoprecipitation to assess the SRM level of WT and mutant β-Catenin in 293 T cells. **d** Quantification of SRM of β-Catenin. ***$p<0.005$. Data represent mean ± SD. **e** Top-flash luciferase assay for WT and mutant β-Catenin in cells transfected as indicated. ***$p<0.005$, one-way ANOVA. Data represent mean ± SD ($n=6$). **f** Representative immunostaining for TCF/LEF;H2B-GFP reporter assay with WT and mutant β-Catenin in 10T1/2 cells. Scale bar: 100 μm. **g** Quantification of GFP-positive cells. Mean values of 400 fields per each group ($n=6$). ***$p<0.001$, one-way ANOVA test. Data represent mean ± SEM. **h** Immunoblot analysis for GFP and β-Catenin as shown in panel (**g**)

PRMT7 methylates β-Catenin at arginine residue at 93 that appears to be critical for the regulation of β-Catenin activity.

Similar to PRMT7, PRMT5 overexpression in rat cardiomyocytes prevented the phenylephrine-induced hypertrophy [40]. However, the molecular mechanisms by which these PRMTs regulate cardiomyocyte hypertrophy differ. While PRMT7 regulates cardiac hypertrophic responses through the β-Catenin function, PRMT5 has been shown to

methylate and inhibit GATA4 activation [40]. Due to the early embryonic lethality in mice lacking PRMT5 [41], its role in cardiac function is currently unknown. Furthermore, PRMT5 has been also implicated in the promotion of Wnt signaling through induction of Disheveled 3 expression [42], unlike the inhibitory role of PRMT7 for Wnt signaling. Since PRMT7-defiecnet hearts exhibited decreased SRM of β-Catenin without altered PRMT5 level, a direct role of PRMT7 in β-Catenin methylation is suggested. However, the fact that both PRMT5 and PRMT7 depletion exacerbates PE-induced hypertrophy while overexpression of either one of these proteins prevents hypertrophy in cardiomyocytes, indicates possible crosstalk between these enzymes. The crosstalk between PRMTs is relatively uncharacterized. One example is the crosstalk at the arginine residue 3 in histone H4 that can be methylated by type I and type II PRMTs modulating gene expression positively and negatively, respectively. Although the precise regulatory mechanism is incompletely characterized, an interplay between PRMTs might be important in gene regulation [38]. In hepatocytes, PRMT1 has been shown to methylate and activate FOXO1 to modulate hepatic glucose metabolism [43], while PRMT1 modulates FOXO3 via PRMT6 expression in skeletal muscle. PRMT1 ablation in skeletal muscle upregulates PRMT6 that in turn methylates and activates FOXO3-mediated autophagy and muscle protein degradation leading to muscle atrophy [39]. Thus, further investigation will be required for elucidation of crosstalk between these PRMTs in diverse biological events.

A recent study has shown that PRMT7 activation augmented the epithelial-mesenchymal transition (EMT) program in breast cancer cells, accompanied by enhanced N-Cadherin and decreased β-Catenin levels [44]. However, the level of N-Cadherin is not greatly altered in PRMT7-deficient cardiac tissues and it is unknown whether PRMT7 directly targets β-Catenin in EMT of breast cancer cells which might modulate cell adhesion. Although the detailed mechanism might differ, yet the β-Catenin downregulation by PRMT7 overexpression is similar in both, cancer cells and cardiomyocytes. Thus, it is conceivable that similar mechanisms might act in control of EMT of breast cancer cells and cardiomyocyte function. Interestingly, some reports suggested that Axin methylation by PRMT1 stabilized Axin and β-Catenin complex, leading to the degradation of β-Catenin [45] and PRMT1 mediated the GSK3 phosphorylation in Wnt signaling pathway for endocytosis [46]. Taken together, the arginine methylation of Wnt effectors by PRMTs might be essential for the regulation and should be investigated.

In summary, our results demonstrate a novel regulatory mechanism whereby arginine methylation affects β-Catenin activity thereby cardiac function. The protective effects of PRMT7 against cardiac remodeling indicate that targeting PRMT7 may provide a novel therapeutic strategy for the treatment of heart failure.

Supplementary Information The online version contains supplementary material available at https://doi.org/10.1007/s00018-021-04097-x.

Acknowledgements This research was supported by the National Research Foundation Grant funded by the Korean Government (MSIP) (NRF-2019R1A2C2006233; NRF-2017M3A9D8048710; 2016R1A5A2945889).

Author contributions BYA, MHJ, JHP, HJJ, TAV, JHB, SA, SWK, YKK, DR, HJK, HC, GUB, and JSK contributed to the experimental design, research and data analysis. BYA, MHJ, GUB, and JSK wrote the manuscript.

Funding This research received no external funding.

Availability of data and material All data related to this work is presented in the paper and its supplements. The materials used in this study are available to any qualified researcher upon reasonable request addressed to J.S.K.

Declarations

Conflict of interest The authors have declared that no conflict of interest exists.

Ethics approval and consent to participate All experimental protocols were approved by the Institutional Animal Care for Ethics and Use Committee of Sunkyunkwan University (SUSM, SKKUIACUC 2018-11-14-2), and the study followed institutional and National Institutes of Health guidelines for laboratory animal care.

Consent for publication Authors, the undersigned, give our consent for the publication of identifiable details, which can include photograph(s) and/or videos and/or case history and/or details within the text ("Material") to be published in the Cellular and Molecular Life Sciences.

References

1. Kehat I, Molkentin JD (2010) Molecular pathways underlying cardiac remodeling during pathophysiological stimulation. Circulation 122:2727–2735
2. Bergmann MW (2010) Wnt signaling in adult cardiac hypertrophy and remodeling: lessons learned from cardiac development. Circ Res 107:1198–1208
3. Baurand A, Zelarayan L, Betney R, Gehrke C, Dunger S, Noack C, Busjahn A, Huelsken J, Taketo MM, Birchmeier W, Dietz R, Bergmann MW (2007) β-Catenin downregulation is required for adaptive cardiac remodeling. Circ Res 100:1353–1362
4. Zhao Y, Wang C, Wang C, Hong X, Miao J, Liao Y, Zhou L, Liu Y (2018) An essential role for Wnt/β-Catenin signaling in mediating hypertensive heart disease. Sci Rep 8:8996
5. Duan J, Gherghe C, Liu D, Hamlett E, Srikantha L, Rodgers L, Regan JN, Rojas M, Willis M, Leask A, Majesky M, Deb A (2012) Wnt1/β-Catenin injury response activates the epicardium and cardiac fibroblasts to promote cardiac repair. EMBO J 31:429–442
6. Angers S, Moon RT (2009) Proximal events in Wnt signal transduction. Nat Rev Mol Cell Biol 10:468477

7. MacDonald BT, Tamai K, He X (2009) Wnt/β-Catenin signaling: components, mechanisms, and diseases. Dev Cell 17:9–26
8. Levy L, Wei Y, Labalette C, Wu Y, Renard C-A, Buendia MA, Neuveut C (2004) Acetylation of β-Catenin by p300 regulates β-Cateni-Tcf4 interaction. Mol Cell Biol 24:3404–3414
9. Krause CD, Yang Z-H, Kim Y-S, Lee J-H, Cook JR, Pestka S (2007) Protein arginine methyltransferases: evolution and assessment of their pharmacological and therapeutic potential. Pharmacol Ther 113:50–87
10. Biggar KK, Li SS (2015) Non-histone protein methylation as a regulator of cellular signalling and function. Nat Rev Mol Cell Biol 16:5–17
11. Liu F, Wan L, Zou H, Pan Z, Zhou W, Lu X (2020) PRMT7 promotes the growth of renal cell carcinoma through modulating the β-Catenin/C-Myc axis. Int J Biochem Cell Biol 120:105686
12. Jeong HJ, Lee HJ, Vuong TA, Choi KS, Choi D, Koo SH, Cho SC, Cho H, Kang JS (2016) PRMT7 deficiency causes reduced skeletal muscle oxidative metabolism and age-related obesity. Diabetes 65:1868–1882
13. Blanc RS, Vogel G, Chen T, Crist C, Richard S (2016) PRMT7 preserves satellite cell regenerative capacity. Cell Rep 14:1528–1539
14. Kernohan KD, McBride A, Xi Y, Martin N, Schwartzentruber J, Dyment DA, Majewski J, Blaser S, Constorium CC, Boycott KM, Chitayat D (2017) Loss of arginine methyltransferase PRMT7 causes syndromic intellectual disability with microcephaly and brachydactyly. Clin Genet 91:708–716
15. Akawi N, McRae J, Ansari M, Balasubramanian M, Blyth M, Brady AF, Clayton S, Cole T, Deshpande C, Fitzgerald TW, Foulds N, Francis R, Gabriel G, Gerety SS, Goodship J, Hobson E, Jones WD, Joss S, King D, Klena N, Kumar A, Lees M, Lelliott C, Lord J, McMullan D, O'Regan M, Osio D, Piombo V, Prigmore E, Rajan D, Rosser E, Sifrim A, Smith A, Swaminathan GJ, Turnpenny P, Whitworth J, Wright C, Firth HV, Barrett JC, Lo CW, FitzPatrick DR, Hurles ME, the DDD study (2015) Discovery of four recessive developmental disorders using probabilistic genotype and phenotype matching among 4,125 families. Nat Genet 47:1363–1369
16. Pyun JH, Kim HJ, Jeong MH, Ahn BY, Vuong TA, Lee DI, Choi S, Koo SH, Cho H, Kang JS (2018) Cardiac specific PRMT1 ablation causes heart failure through CAMKII dysregulation. Nat Commun 9:5107
17. Murata K, Lu W, Hashimoto M, Ono N, Muratani M, Nishikata K, Kim JD, Ebilhara S, Ishida J, Fukamizu A (2018) PRMT1 deficiency in mouse juvenile heart induces dilated cardiomyopathy and reveals cryptic alternative splicing products. iScience 8:200–213
18. Cassis LA, Marshall DE, Fettinger MJ, Rosenbluth B, Lodder RA (1998) Mechanisms contributing to angiotensin II regulation of body weight. Am J Physiol 274:E867–E876
19. Olivares-Silva F, Gregorio ND, Espitia-Corredor J, Espinoza C, Vivar R, Silva D, Osorio JM, Lavandero S, Peiro C, Sanchez-Ferrer C, Diaz-Araya G (2021) Resolvin-D1 attenuation of angiotensin II-induced cardiac inflammation in mice is associated with prevention of cardiac remodeling and hypertension. Biochim Biophys Acta Mol Basis Dis 1867:166241
20. Lee SJ, Hwang J, Jeong HJ, Yoo M, Go GY, Lee JR, Leem YE, Park JW, Seo DW, Kim YK, Hahn MJ, Han JW, Kang JS, Bae GU (2016) PKN2 and Cdo interact to activate AKT and promote myoblast differentiation. Cell Death Dis 7:e2431
21. Jeong MH, Kim HJ, Pyun JH, Choi KS, Lee DI, Solhjoo S, O'Rourke B, Tomaselli GF, Jeong DS, Cho H, Kang JS (2017) Cdon deficiency causes cardiac remodeling through hyperactivation of Wnt/ζ-Catenin signaling. Proc Natl Acad Sci U S A 114:E1345–E1354
22. Jeong MH, Ho SM, Vuong TA, Jo SB, Liu G, Aaronson SA, Leem YE, Kang JS (2014) Cdo suppresses canonical Wnt signalling via interaction with Lrp6 thereby promoting neuronal differentiation. Nat Commun 5:5455
23. Leem YE, Jeong HJ, Kim HJ, Koh J, Kang KJ, Bae GU, Cho H, Kang JS (2016) Cdo regulates surface expression of Kir2.1 K+ channel in myoblast differentiation. PLoS ONE 11:e0158707
24. Vuong TA, Jeong HJ, Lee HJ, Kim BG, Leem YE, Cho H, Kang JS (2020) PRMT7 methylates and suppresses GLI2 binding to SUFU thereby promoting its activation. Cell Death Differ 27:15–28
25. Kwon YR, Jeong MH, Leem YE, Lee SJ, Kim HJ, Bae GU, Kang JS (2014) The Shh coreceptor Cdo is required for differentiation of midbrain dopaminergic neurons. Stem Cell Res 13:262–274
26. Lee HJ, Jo SB, Romer AI, Lim HJ, Kim MJ, Koo SH, Krauss RS, Kang JS (2015) Overweight in mice and enhanced adipogenesis in vitro are associated with lack of the hedgehog coreceptor Boc. Diabetes 64:2092–2103
27. Jeong MH, Leem YE, Kim HJ, Kang K, Cho H, Kang JS (2016) A Shh coreceptor Cdo is required for efficient cardiomyogenesis of pluripotent stem cells. J Mol Cell Cardiol 93:57–66
28. Vuong TA, Leem YE, Kimg BG, Cho H, Lee SJ, Bae GU, Kang JS (2017) A Sonic hedgehog coreceptor, BOC regulates neuronal differentiation and neurite outgrowth via interaction with ABL and JNK activation. Cell Signal 30:30–40
29. Yousefi F, Shabaninejad Z, Vakili S, Derakhshan M, Movahedpour A, Dabiri H, Ghasemi Y, Mahjoubin-Tehran M, Nikoozadeh A, Savardashtaki A, Mirzaei H, Hamblin MR (2020) TGF-β and Wnt signaling pathways in cardiac fibrosis: non-coding RNAs come into focus. Cell Commun Signal 18:87
30. Garcia-Hoz C, Sanchez-Fernandez G, Garcia-Escudero R, Fernandez-Velasco M, Palacios-Garcia J, Ruiz-Meana M, Diaz-Meco MT, Leitges M, Moscat J, Garcia-Dorado D, Bosca L, Major F Jr, Ribas C (2012) Protein kinase C (PKC)ζ-mediated Gαq stimulation of ERK5 protein pathway in cardiomyocytes and cardiac fibroblasts. J Biol Chem 287:7792–7802
31. Feng Y, Maity R, Whitelegge JP, Hadjikyriacou A, Li Z, Zurita-Lopez C, Al-Hadid Q, Clark AT, Bedford MT, Masson JY, Clarke SG (2013) Mammalian protein arginine methyltransferase (PRMT7) specifically targets RXR sites in lysine- and arginine-rich regions. J Biol Chem 288:37010–37025
32. Onwuli DO, Rigau-Roca L, Cawthorne C, Beltran-Alvarez P (2017) mapping arginine methylation in the human body and cardiac disease. Proteomics Clin Appl 11:1600106
33. Nakamura M, Sadoshima J (2018) Mechanisms of physiological and pathological cardiac hypertrophy. Nat Rev Cardiol 15:387–407
34. Nomura N, Tani T, Konda T, Kim K, Kitai T, Nomoto N, Suganuma N, Nakamura H, Sumida T, Fujii Y, Kawai J, Kaji S, Furukawa Y (2018) Significance of isolated papillary muscle hypertrophy: a comparison of left ventricular hypertrophy diagnosed using electrocardiography vs echocardiography. Echocardiography 35:292–300
35. Sheehy SP, Huang S, Parker KK (2009) Time-warped comparison of gene expression in adaptive and maladaptive cardiac hypertrophy. Cir Cardiovasc Genet 2:116–124
36. Malekar P, Hagenmueller M, Anyanwu A, Buss S, Streit MR, Weiss CS, Wolf D, Riffel J, Bauer A, Katus HA, Hardt SE (2010) Wnt signaling is critical for maladaptive cardiac hypertrophy and accelerates myocardial remodeling. Hypertension 55:939–945
37. Yu L, Meng W, Ding J, Cheng M (2016) Klotho inhibits angiotensin II-induced cardiomyocytes hypertrophy through suppression of the AT1R/β-Catenin pathway. Biochem Biophys Res Commun 473:455–461
38. Dhar S, Vemulapalli V, Patananan AN, Huang GL, Lorenzo AD, Richard S, Comb MJ, Guo A, Clarke SG, Bedford MT (2013)

Loss of the major type I arginine methyltransferase PRMT1 causes substrate scavenging by other PRMTs. Sci Rep 3:1311
39. Choi S, Jeong HJ, Kim H, Choi D, Cho SC, Seong JK, Koo SH, Kang JS (2019) Skeletal muscle-specific PRMT1 deletion causes muscle atrophy via deregulation of the PRMT6-FOXO3 axis. Autophagy 15:1069–1081
40. Chen M, Yi B, Sun J (2014) Inhibition of cardiomyocyte hypertrophy by protein arginine methyltransferase 5. J Biol Chem 289:24325–24335
41. Tee WW, Pardo M, Theunissen TW, Yu L, Choudhary JS, Hajkova P, Surani MA (2010) PRMT5 is essential for early mouse development and acts in the cytoplasm to maintain ES cell pluripotency. Genes Dev 24:2772–2777
42. Jin Y, Zhou J, Xu F, Jin B, Cui L, Wang U, Du X, Li J, Li P, Ren R, Pan J (2016) Targeting methyltransferase PRMT5 eliminates leukemia stem cells in chronic myelogenous leukemia. J Clin Invest 126:3961–3980
43. Choi D, Oh KJ, Han HS, Yoon YS, Jung CY, Kim ST, Koo SH (2012) Protein arginine methyltransferase 1 regulates hepatic glucose production in a FoxO1-dependent manner. Hepatology 56:1546–1556
44. Geng P, Zhang Y, Liu X, Zhang N, Liu Y, Liu X, Lin C, Yan X, Li Z, Wang G, Li Y, Tan J, Liu DX, Huang B, Lu J (2017) Automethylation of protein arginine methyltransferase 7 and its impact on breast cancer progression. FASEB J 31:2287–2300
45. Cha B, Kim W, Kim YK, Hwan BN, Park SY, Yoon JW, Par WS, Cho JW, Bedford MT, Jho EH (2011) Methylation by protein arginine methyltransferase 1 increases stability of Axin, a negative regulator of Wnt signaling. Oncogene 30:2379–2389
46. Albrecht LV, Ploper D, Tejeda-Munoz N, Robertis EMD (2018) Arginine methylation is required for canonical Wnt signaling and endolysosomal trafficking. Proc Natl Acad Sci U S A 115:E5317–E5325